Expression of Peroxisome Proliferator-activated Receptors α, ß, γ, and H- and L-Prostaglandin D Synthase During Osteoarthritis in the Spontaneous Hartley Guinea Pig and Experimental Dog Models

Sarah-Salwa Nebbaki, Fatima Ezzahra El Mansouri, Hassan Afif, Mohit Kapoor, Mohamed Benderdour, Jean-Pierre Pelletier, Johanne Martel-Pelletier, and Hassan Fahmi

ABSTRACT. ***Objective.*** To investigate the expression of peroxisome proliferator-activated receptors (PPAR) α, β, and γ, and hematopoietic and lipocalin-type prostaglandin D synthase (H- and L-PGDS) over the course of osteoarthritis (OA) in the spontaneous Hartley guinea pig and the anterior cruciate ligament transection dog models.

Methods. Guinea pigs were sacrificed at 2 (control group), 4, 8, and 12 months of age (n = 5 per group). Non-operated (control) and operated dogs were sacrificed at 4, 8, and 12 weeks postsurgery. Cartilage was evaluated histologically using the Osteoarthritis Research Society International (OARSI) guidelines. The expression of PPAR-α, β, γ, and H- and L-PGDS was evaluated by real-time PCR and immunohistochemistry. The nonparametric Spearman test was used for correlation analysis.

Results. PPAR-α, β, and γ were detected in medial tibial plateau from control animals in both the spontaneous and surgical models. Levels of PPAR-α and β did not change over the course of OA, whereas PPAR-γ levels decreased during progression of disease. We also observed that the expression of H-PGDS remained unchanged, whereas L-PGDS increased over the course of OA. PPAR-γ levels correlated negatively, whereas L-PGDS levels correlated positively, with the histological score of OA.

Conclusion. The level of PPAR-γ decreased, whereas level of L-PGDS increased during the progression of OA. These data suggest that reduced expression of PPAR-γ may contribute to the pathogenesis of OA, whereas enhanced expression of L-PGDS may be part of a reparative process. (First Release April 1 2013; J Rheumatol 2013;40:877–90; doi:10.3899/jrheum.120738)

Key Indexing Terms:
PEROXISOME PROLIFERATOR-ACTIVATED RECEPTORS
PROSTAGLANDIN D SYNTHASE
CARTILAGE
OSTEOARTHRITIS

Osteoarthritis (OA) is the most common form of joint disorder worldwide and is frequently associated with pain and functional impairment. OA is characterized by articular cartilage degradation, synovitis, and subchondral bone remodeling[1,2,3]. Although the precise etiology of OA is not known, the proinflammatory cytokines such as interleukin 1β (IL-1β) and tumor necrosis factor-α (TNF-α) are believed to play a pivotal role in pathogenesis[1,2,3]. One mechanism by which IL-1 exerts its effects is by inducing articular cell tissues to produce several mediators known for their role in articular inflammation and destruction, including matrix metalloproteinases (MMP), aggrecanases, inducible nitric oxide (iNOS), cyclooxygenase-2 (COX-2), and microsomal prostaglandin E-synthase-1 (mPGES-1)[1,2,3].

Peroxisome proliferator-activated receptors (PPAR) are ligand-activated transcription factors and members of the nuclear hormone receptor superfamily, which include receptors for steroids, thyroid hormone, vitamin D, and retinoic acid. Three PPAR isoforms have been described: PPAR-α, PPAR-β/δ, and PPAR-γ[4]. PPAR-α is mostly present in liver, heart, and muscle, and is believed to function in the catabolism of fatty acid[5]. PPAR-β/δ is expressed ubiquitously, and is involved in lipid homeostasis,

From the Osteoarthritis Research Unit, University of Montreal Hospital Research Center (CRCHUM), Notre-Dame Hospital, Montréal, Québec, Canada.

Supported by the Canadian Institutes of Health Research (CIHR) Grant MOP-84282 and The Arthritis Society. F.E. El Mansouri was supported by a fellowship from the CIHR Training on Mobility and Posture Deficiencies.

S-S. Nebbaki, MSc; F.E. El Mansouri, MSc; H. Afif, PhD; M. Kapoor, PhD; J. Martel-Pelletier, PhD; J-P. Pelletier, MD; H. Fahmi, PhD, Osteoarthritis Research Unit, CRCHUM; M. Benderdour, PhD, Research Centre, Sacré-Coeur Hospital, Montreal.

Address correspondence to H. Fahmi, Osteoarthritis Research Unit, Centre hospitalier de l'Université de Montréal, Hôpital Notre-Dame, 1560 rue Sherbrooke est, Montréal, Québec H2L 4M1, Canada. E-mail: h.fahmi@umontreal.ca

Accepted for publication February 4, 2013.

epidermal maturation, wound healing, and brain development[6,7]. PPAR-γ is the most intensively studied form. It is expressed in a broad range of tissues and plays pivotal roles in various physiological and pathological processes, including the regulation of glucid and lipid metabolism, inflammation[8], and diabetes[9]. In addition, increasing evidence suggests that PPAR-γ plays an important role in the pathogenesis of OA and possibly other chronic arthritic diseases[10].

PPAR-γ can be activated by a variety of naturally occurring compounds including the cyclopentanone prostaglandin 15-deoxy-$\Delta^{12,14}$-prostaglandin J_2 (15d-PGJ_2), the most potent endogenous ligand for PPAR-γ to date[11,12]. Dehydration of PGD_2 generates 15d-PGJ_2. The biosynthesis of PGD_2 is catalyzed by 2 PGD synthases (PGDS): one is glutathione-independent, the lipocalin-type PGDS (L-PGDS), and the other is glutathione-dependent, the hematopoietic PGDS (H-PGDS)[13].

Several studies have shown that PPAR-γ is expressed and functional in cartilage and that PPAR-γ agonists downregulate inflammatory responses in chondrocytes. For instance, PPAR-γ agonists suppress IL-1-induced iNOS, COX-2, and mPGES-1 expression as well as NO and PGE_2 production in human and rat chondrocytes[14,15,16,17,18,19,20,21]. In addition to their antiinflammatory effects, PPAR-γ activators were also reported to downregulate catabolic responses in articular chondrocytes. Indeed, PPAR-γ activators prevent the induction of several MMP including MMP-1, -3, -9, and -13, which play important roles in cartilage degradation[22,23,24,25]. In support of the protective effects of PPAR-γ agonists in OA, we have demonstrated that PPAR-γ activators reduce the symptoms and severity of the disease in canine[26] and guinea pig[27] models.

Although the protective effects of the PPAR-γ pathway in OA have been well documented, little information is available on its expression in cartilage during the course of the disease. We investigated the expression of PPAR-α, β, and γ, and H- and L-PGDS in cartilage during progression of OA in the spontaneous Hartley guinea pig model and anterior cruciate ligament transection (ACLT) dog model.

MATERIALS AND METHODS

Animals. Male Hartley guinea pigs aged 2, 4, 8, and 12 months (n = 5 each) were purchased (Charles River Laboratories). Animals were housed in standard guinea pig cages and fed standard guinea pig chow containing vitamin C (1 mg/g), vitamin D3 (3.4 IU/g), and water *ad libitum*. Animals were acclimated to housing conditions for 1 week prior to experiments. Guinea pigs were euthanized by intraperitoneal injection of barbiturate.

Seventeen adult crossbred dogs (age 2 to 3 yrs), each weighing 20 to 25 kg, were used in this study. OA was induced in 12 dogs by surgical sectioning of the ACL of the right knee through a stab incision as described[28]. The animals were operated on under general anesthesia with phenobarbital sodium (25 mg/kg). After surgery, the dogs were housed on a farm where they could exercise *ad libitum* under supervision to ensure that they were bearing weight on the operated knee. Dogs were sacrificed at 4 weeks (n = 4), 8 weeks (n = 4), or 12 weeks (n = 4) after surgery by intravenous barbiturate overdose injection. Non-operated normal dogs (n = 5) were used as a baseline control and were subjected to the same housing and exercise conditions. All aspects of this study were approved by the local Institutional Committee for Animal Protection.

Tissue preparation and histological analysis. Guinea pig knee joints were harvested and fixed with TissuFix #2 (Chaptec). Tissues were rinsed with phosphate buffered saline (PBS), decalcified in 5% formic acid for 5 days (2-mo-old animals), 7 days (4-mo-old), 14 days (8-mo-old), and 35 days (12-mo-old). Paraffin sections (5 μm) of the whole joint (5–10 sections per knee) were stained with Safranin-O and histological grading was performed independently by 2 blinded observers (SSN and FEE) according to the Osteoarthritis Research Society International (OARSI) scoring system[29]. This scale evaluates the severity of OA lesions based on cartilage structure (scale 0–8), proteoglycan content (scale 0–6), cellularity (scale 0–3), and tidemark integrity (0–1).

The right knee of each dog was placed on ice and dissected. Five specimens of cartilage were removed from fixed predefined locations of the weight-bearing areas of the medial tibial plateaus. Specimens from normal dogs were obtained from the same anatomical sites. Cartilage specimens were fixed in TissuFix #2, embedded in paraffin, and 5 μm sections prepared. Serial sections (5–10 sections per specimen) were stained with Safranin-O and histological grading was performed independently by 2 blinded observers (SSN and FEE), following OARSI guidelines[30]. This scale evaluates the severity of OA lesions based on cartilage structure (0–12), cellular changes (0–12), proteoglycan staining (0–12), and collagen integrity (0–9).

Immunohistochemistry. The following antibodies were used: anti-PPAR-α (sc-9000; Santa Cruz Biochemical); anti-PPAR-β (sc7197; Santa Cruz Biochemical); anti-PPAR-γ (sc-7196; Santa Cruz Biochemical); anti-H-PGDS (catalog no. 160013; Cayman Chemical); and anti-L-PGDS (catalog no. 160003; Cayman Chemical).

Five to 10 sections of whole guinea pig knee joints or cartilage samples from weight-bearing areas of the tibial plateau of dogs were processed for immunohistochemistry as described[26,31]. Briefly, paraffin sections (5 μm) were deparaffinized in toluene and dehydrated in a graded ethanol series. Specimens were then preincubated with chondroitinase avidin-biotin complex (0.25 U/ml in PBS pH 8.0) for 60 min at 37°C, followed by 30 min incubation with Triton X-100 (0.3%) at room temperature. Slides were then washed in PBS followed by 2% hydrogen peroxide/methanol for 15 min. They were incubated further for 60 min with 2% normal serum (Vector Laboratories) and overlaid with primary antibody for 18 h at 4°C in a humidified chamber. Each slide was washed 3 times in PBS pH 7.4 and stained using the avidin-biotin complex method (Vectastain ABC kit; Vector Laboratories). The color was developed with 3,3'-diaminobenzidine (DAB; Vector Laboratories) containing hydrogen peroxide and nickel chloride. The slides were counterstained with eosin. The specificity of staining was evaluated using an antibody that had been preadsorbed (1 h, 37°C) with a 20-fold molar excess of the blocking peptide, and by substituting the primary antibody with nonimmune rabbit IgG (Chemicon), at the same concentration as the primary antibody. Evaluation of positive-staining chondrocytes in the central region of the guinea pig joint or cartilage samples from dogs was performed using our method[26,31]. For each specimen, 6 microscopic fields were examined under 40H magnification. The total number of chondrocytes and the number of chondrocytes staining positive were evaluated and results were expressed as the percentage of chondrocytes staining positive (cell score).

RNA extraction and reverse transcription-PCR. Cartilage samples were dissected from medial tibial plateaus of guinea pigs or from weight-bearing areas of tibial plateaus of dogs, and total RNA was isolated using TRIzol® reagent (Invitrogen), according to the manufacturer's instructions. To remove contaminating DNA, isolated RNA was treated with RNase-free DNase I (Ambion). The RNA was quantitated using the RiboGreen RNA quantitation kit (Molecular Probes), dissolved in diethylpyrocarbonate (DEPC)-treated H_2O, and stored at –80°C until use. One microgram of total

RNA was reverse-transcribed using the Moloney Murine Leukemia Virus reverse transcription (Fermentas) as detailed in the manufacturer's guidelines. One-fiftieth of the reverse transcription reaction was analyzed by real-time PCR as described below.

The following primers were used for guinea pig genes: PPAR-α, sense, 5'-TCA TCA CAG ATA CCC TGT CC-3' and antisense, 5'-CGG TTC TTT TTC TGG ATC TT-3'; PPAR-β, sense, 5'-CTC CAG CAG TTA CAC AGA CC-3' and antisense, 5'-GCA GTA CTG GCA CTT GTT TC-3'; PPAR-γ, sense, 5'-AAG CCG TGC AAG AGA TCA CAG AGT-3' and antisense, 5'-TCT CGT GCA CAC CAT ACT TGA GCA-3'; H-PGDS, sense, 5'-TCA ATA TGA GAG GGA GAG CA-3' and antisense, 5'-AGT CCA TCC ACT TCC AAA AT-3'; L-PGDS, sense, 5'-ATA AGT GCC TGA AGG AGG AG-3' and antisense, 5'-TCT CAG GTC TGC AGT GAA GT-3'; and glyceraldehyde-3-phosphate dehydrogenase (GAPDH), sense, 5'-ACC TGC CGC CTG GAG AA-3' and antisense, 5'-CCC TCT GAT GCC TGC TTC AC-3'; or dog genes: PPAR-α, sense, 5'-AAT GCA CTG GAG CTA GAT GA-3' and antisense, 5'-GAA GGA GTT TTG GGA AGA GA-3'; PPAR-β, sense, 5'-GCA TGA AGC TGG AAT ATG AG-3' and antisense, 5'-TTT TTC AGG TAG GCG TTG TA-3'; PPAR-γ, sense, 5'-TCA CAG AGT ACG CCA AAA GT-3' and antisense, 5'-ACT CCC TTG TCA TGA ATC CT-3'; H-PGDS, sense, 5'-TTT AAT ATG AGG GGG AGA GC-3' and antisense, 5'-GGC TCT GG GAA GGT TAA GT-3'; L-PGDS, sense, 5'-ACT GCT CTG CTC TTT CCT CT-3' and antisense 5'-GAT TTG CTT CCG GAG TTT AT-3'; and GAPDH, sense, 5'-AGG CTG TGG GCA AGG TCA TC-3' and antisense, 5'-AAG GTG GAA GAG TGG GTG T-3'.

Real-time PCR. Real-time PCR analysis was performed in a total volume of 50 μl containing template DNA, 200 nM of sense and antisense primers, 25 μl of SYBR® Green master mix (Qiagen), and uracyl-N-glycosylase (UNG; 0.5 unit; Epicenter Technologies). After incubation at 50°C for 2 min (UNG reaction) and 95°C for 10 min (UNG inactivation and activation of AmpliTaq Gold enzyme), the mixtures were subjected to 40 amplification cycles (15 s at 95°C for denaturation, 1 min for annealing, and extension at 60°C). Incorporation of SYBR® Green dye into PCR products was monitored in real time using a GeneAmp 5700 Sequence Detection System (Applied Biosystems), allowing determination of the threshold cycle (CT) at which exponential amplification of PCR products begins. After PCR, dissociation curves were generated with 1 peak, indicating the specificity of the amplification. A CT value was obtained from each amplification curve using the software provided by the manufacturer.

Relative messenger RNA (mRNA) expression in chondrocytes was determined using the ΔΔCT method, as detailed in the manufacturer's guidelines (Applied Biosystems). A ΔCT value was first calculated by subtracting the CT value for the housekeeping gene GAPDH from the CT value for the gene of interest. A ΔΔCT value was then calculated by subtracting the ΔCT value of the control (unstimulated cells) from the ΔCT value of each treatment. Fold changes compared with the control were then determined by raising 2 to the –ΔΔCT power. Each PCR generated only the expected specific amplicon, as shown by the melting-temperature profiles of the final product and by gel electrophoresis of test PCR. Each PCR was performed in triplicate on 2 separate occasions for each independent experiment.

Human chondrocyte culture. Human OA cartilage was obtained from patients undergoing total knee replacement (n = 6, mean age 62 ± SD 8 yrs). All patients with OA were diagnosed on criteria developed by the American College of Rheumatology Diagnostic Subcommittee for OA. At the time of surgery, the patients had symptomatic disease requiring medical treatment in the form of nonsteroidal antiinflammatory drugs or selective COX-2 inhibitors. Patients who had received intraarticular steroid injections were excluded. The Clinical Research Ethics Committee of our institution approved the study protocol and informed consent was obtained from each donor. Chondrocytes were released from cartilage by sequential enzymatic digestion as described[14,25].

Transient transfection. The expression vector for human L-PGDS was kindly provided by Dr. K. Fujimori (University of Pharmaceutical Sciences, Osaka, Japan)[32]. Transient transfection experiments were performed using the FuGene-6 transfection reagent according to the manufacturer's recommended protocol (Roche Applied Science). Briefly, chondrocytes were seeded 24 h prior to transfection at a density of 3×10^5 cells/well in 12-well plates and transiently transfected with 1 μg of the parental empty plasmid (pFLAG-CMV-5a) or the L-PGDS expression plasmid (FLAG-tagged L-PGDS). Eight hours later, the medium was replaced with Dulbecco modified Eagle's medium containing 1% fetal calf serum. At 48 h after transfection, the cells were left untreated or were treated with human recombinant IL-1 (Genzyme) for 24 h. Supernatants were harvested and analyzed for NO and MMP-13 levels. The cells were washed twice in ice-cold PBS and crude extracts were prepared and analyzed by Western blotting with anti-Flag (Sigma) and anti-L-PGDS antibodies as described[14,25].

RNA interference. Specific small interfering RNA (siRNA) for PPAR-γ or scrambled control siRNA were obtained from Dharmacon Inc. Chondrocytes were seeded in 6-well plates at 6×10^5 cells/well and incubated 24 h. Cells were transfected with 100 nM siRNA using the HiPerFect Transfection Reagent (Qiagen) following the manufacturer's recommendations. The medium was changed 24 h later and cells were incubated an additional 24 h before stimulation with 100 pg/ml IL-1 for 24 h. PPAR-γ silencing was evaluated by Western blotting as described[14,25].

NO and MMP-13 determinations. Nitrite levels in conditioned media used as an indicator of NO production were determined using the Griess assay as described[14,25]. Levels of MMP-13 in conditioned media were determined by specific ELISA (R&D Systems). All measurements were performed in duplicate.

Statistical analysis. Statistical analyses were performed using SPSS V.13 (SPSS). Data are expressed as the mean ± SD. Statistical significance was assessed by 2-tailed Student t test. P values < 0.05 were considered statistically significant. The nonparametric Spearman test was used to calculate the correlation between the levels of PPAR-γ and L-PGDS and histological score for OA.

RESULTS

Histological findings. Representative safranin-O-stained sections from 2-, 4-, 8-, and 12-month-old Hartley guinea pig medial tibial plateau articular cartilage are shown in Figure 1A-1D. We focused on this area because it is the site of the earliest OA and reproducible lesions in this model[33,34,35]. At 2 months of age, the articular cartilage was morphologically normal with a smooth surface (Figure 1A). As guinea pigs became older they developed osteoarthritic lesions. By 4 months of age, the cartilage exhibited minor surface irregularity, with decreased safranin-O staining (Figure 1B). By 8 months, surface erosions were readily detected, both cellularity and safranin-O staining were markedly reduced (Figure 1C), and osteophytes began to develop (results not shown). By 12 months, surface erosion became more severe, accompanied by an increase in proteoglycan loss, osteophyte formation, and subchondral bone sclerosis (Figure 1D).

Representative sections of cartilage from normal non-operated dogs, and from experimental animals at 4, 8, and 12 weeks postsurgery are shown in Figure 2A-2D. The articular cartilage from normal (non-operated) dogs demonstrated a normal histological appearance (Figure 2A). At 4 weeks postsurgery, histological changes were made evident by loss of surface integrity, hypocellularity, fibrillations, and

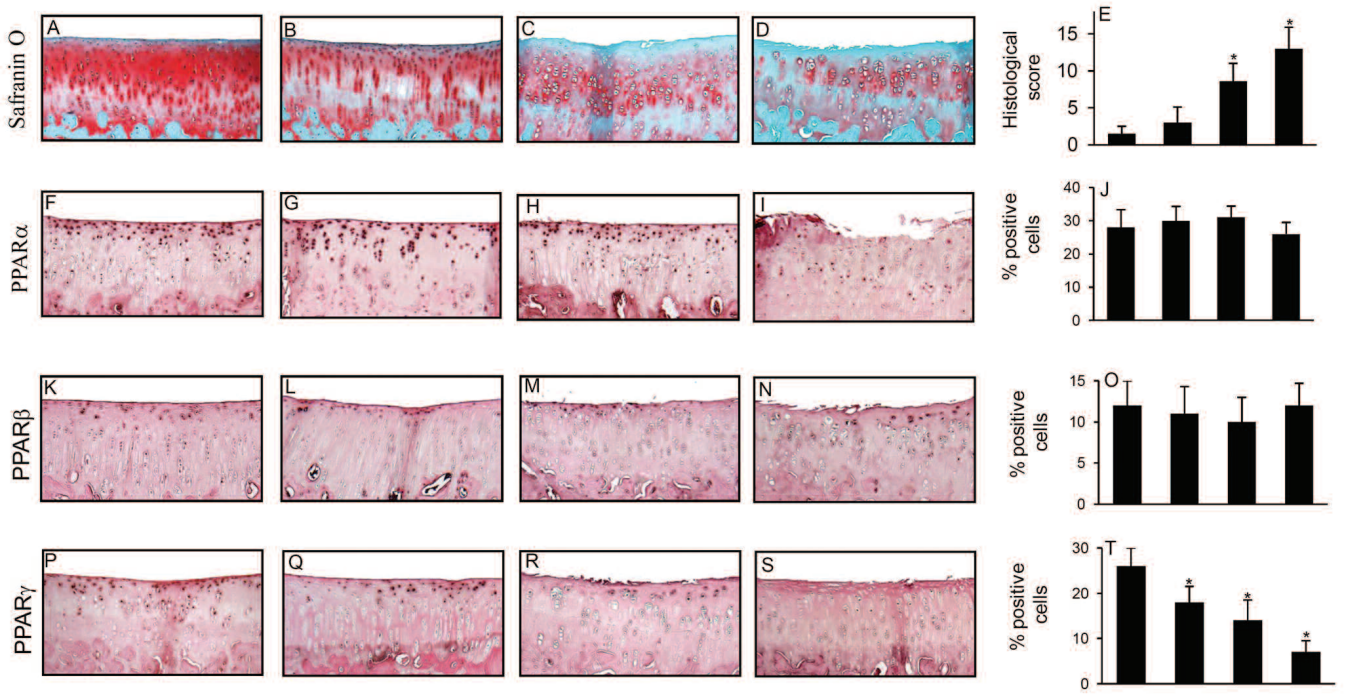

Figure 1. PPAR-α, PPAR-β, and PPAR-γ expression during the course of osteoarthritis (OA) in the Hartley guinea pig model. Knee joint sections from 2-, 4-, 8-, and 12-month-old guinea pigs were stained with safranin-O (A, B, C, D) or analyzed by immunohistochemistry for PPAR-α (F, G, H, I), PPAR-β (K, L, M, N), and PPAR-γ (P, Q, R, S). Control for immunostaining included preadsorbing the primary antibodies with a 20-fold molar excess of immunizing antigen, and substituting the primary antibody with nonimmune rabbit IgG (not shown). E. Mean histological score of OA in the medial tibial plateau. J, O, T. Percentage of chondrocytes expressing PPAR-α, β, and γ during progression of OA in the Hartley guinea pig model. Results are mean ± SD of evaluations of 5 to 10 sections taken from the central region of 5 separate animals. *$p < 0.05$ compared with cartilage from 2-month-old guinea pigs (control). PPAR: peroxisome proliferator-activated receptors.

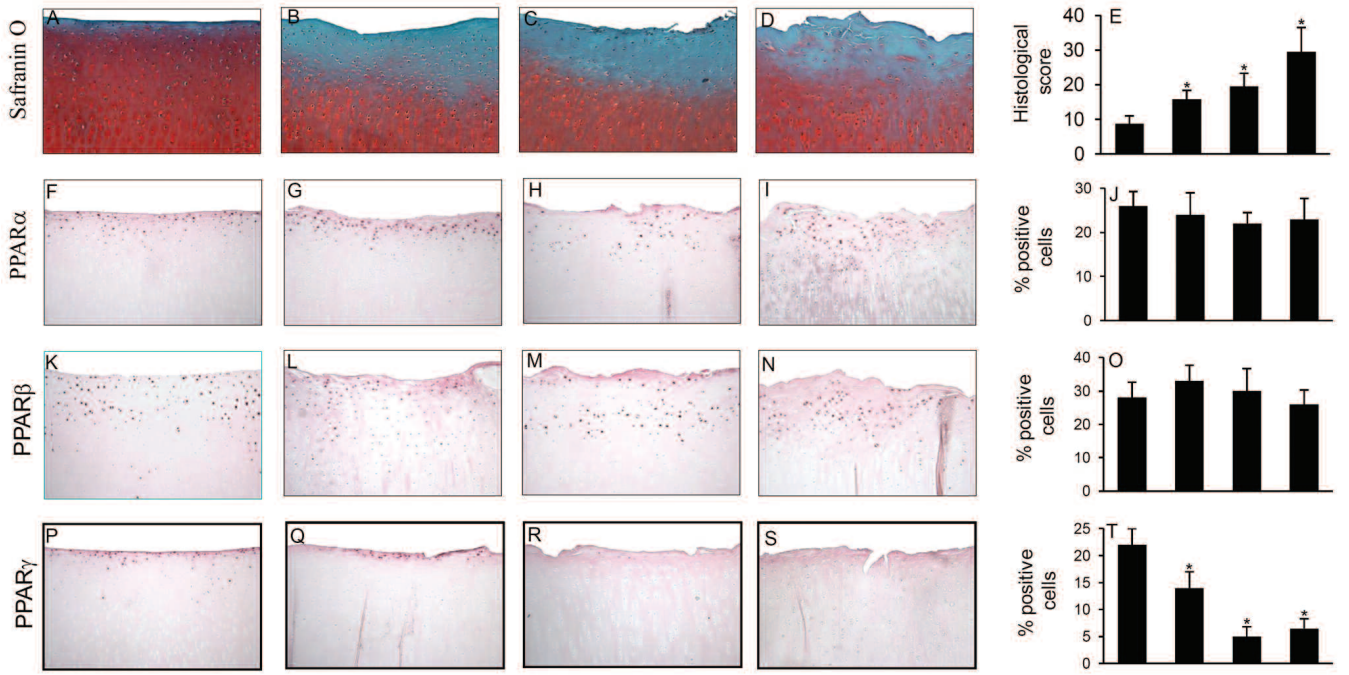

Figure 2. PPAR-α, PPAR-β, and PPAR-γ expression in cartilage during the progression of osteoarthritis (OA) in the ACLT dog model. Cartilage sections from weight-bearing areas of tibial plateaus of normal (control) and operated dogs at 4, 8, 10, and 12 weeks postsurgery were stained with safranin-O (A, B, C, D) or analyzed by immunohistochemistry for PPAR-α (F, G, H, I), PPAR-β (K, L, M, N), and PPAR-γ (P, Q, R, S). Control for immunostaining included preadsorbing the primary antibodies with 20-fold molar excess of immunizing antigen, and substituting the primary antibody with nonimmune rabbit IgG (not shown). E. Mean histological score of OA in the medial tibial plateau. J, O, T. Percentage of chondrocytes expressing PPAR-α, β, and γ during progression of OA in the ACLT dog model. Results are mean ± SD of evaluation of 5 to 10 sections taken from 4 separate animals. *$p < 0.05$ compared with cartilage from non-operated dogs (control). PPAR: peroxisome proliferator-activated receptors; ACLT: anterior cruciate ligament transection.

developing osteophytes (Figure 2B). These changes worsened throughout the course of the disease (Figure 2C, 2D), with the most severe lesions occurring at 12 weeks postsurgery.

Expression of PPAR-α, β, and γ during progression of OA in the spontaneous Hartley guinea pig model. We performed immunohistochemistry to evaluate the expression of PPAR-α, β, and γ in knee joint cartilage from 2-, 4-, 8-, and 12-month-old guinea pigs. As shown in Figure 1F-1I, PPAR-α was detected in all zones of the articular cartilage, and levels were relatively high in the superficial and middle zones. PPAR-β was located essentially in the superficial and middle zones of the cartilage and was expressed at low levels, compared to PPAR-α (Figure 1K-1N). No significant changes were detected for levels of PPAR-α or PPAR-β at any time analyzed (Figure 1F-1I and 1K-1N). The specificity of staining was confirmed using antibodies that had been preadsorbed (1 h, 37°C) with a 20-fold molar excess of the immunizing peptides or nonimmune control IgG (data not shown).

In contrast to PPAR-α and β, PPAR-γ expression varied with age and disease progression (Figure 1P-1S). At 2 months of age, the staining was prominent in both superficial and middle zones of the cartilage (Figure 1P). At 4 months of age, there was a decrease in PPAR-γ staining throughout both superficial and middle zones of the cartilage (Figure 1Q). At 8 months of age, PPAR-γ expression was significantly reduced in both the superficial and middle zones compared with cartilage from 4-month-old animals (Figure 1R). In 12-month-old animals, PPAR-γ expression decreased further (Figure 1S). The decrease tended to be more marked in the superficial zone of the cartilage (Figure 1S). Preincubation of the antibody with the immunizing peptide abolished the staining (data not shown).

Next, we performed real-time PCR analyses to determine whether the observed changes at the protein levels were paralleled by changes at the mRNA levels. mRNA gene expression was evaluated as percentage over control (2-month-old animals) after normalization to the internal control gene, GAPDH. Consistent with the changes at the protein levels, the levels of PPAR-α and PPAR-β mRNA did not change during the course of OA, whereas the level of PPAR-γ mRNA decreased during the progression of OA (Figure 3). Hence, the expression level of PPAR-γ in cartilage changed as OA progressed in the Hartley guinea pig model.

Expression of H- and L-PGDS during progression of OA in the spontaneous Hartley guinea pig model. Next, we analyzed the expression of H- and L-PGDS, which catalyze the biosynthesis of 15d-PGJ_2, the most potent endogenous activator of PPAR-γ. Our results showed both H-PGDS and L-PGDS were present in control cartilage (Figure 4A, 4F). The expression levels of H-PGDS did not change significantly during the course of OA (Figure 4A-4D). In contrast, the levels of L-PGDS varied with age and disease progression (Figure 4F-4I). At 2 months of age, L-PGDS was moderately expressed in the superficial and middle zones (Figure 4A) and increased ~ 2-fold at 4 months of age (Figure 4B). At 8 months of age, L-PGDS levels continued to increase in both superficial and middle zones of cartilage (Figure 4C). By 12 months of age, the staining was further enhanced compared to that of 8-month-old sections, specifically in the deep zone (Figure 4D). The specificity of the staining was confirmed using antibodies that had been preadsorbed (1 hour, 37°C) with a 20-fold molar excess of the immunizing peptides or nonimmune control IgG (data not shown). Similar to levels of H- and L-PGDS protein, the levels of L-PGDS increased with the progression of OA, whereas levels of H-PGDS remained unchanged (Figure 5).

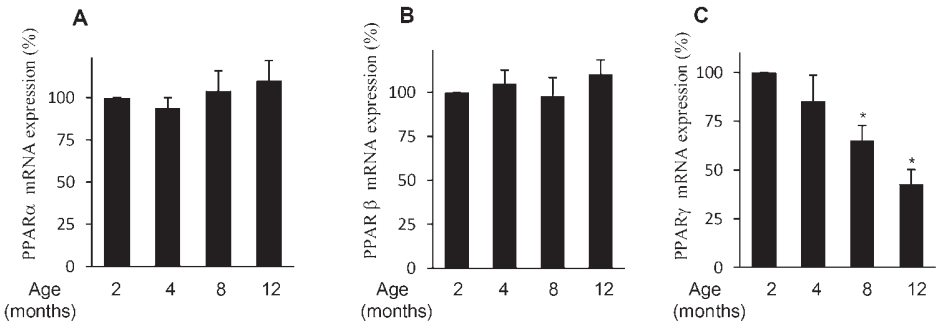

Figure 3. PPAR-α, PPAR-β, and PPAR-γ mRNA expression during the course of osteoarthritis (OA) in the Hartley guinea pig model. Cartilage samples were dissected from medial tibial plateaus of 2-, 4-, 8-, and 12-month-old guinea pigs. Total RNA was isolated, reverse transcribed into cDNA, and PPAR-α (A), PPAR-β (B), PPAR-γ (C), and GAPDH mRNA expression was quantified using real-time PCR. All experiments were performed in triplicate and negative controls without template RNA were included in each experiment. Results are expressed as percentage of control (2-mo-old guinea pigs) and are the mean ± SD from 5 separate animals. *$p < 0.05$ compared with cartilage from 2-month-old guinea pigs (control). PPAR: peroxisome proliferator-activated receptors; GAPDH: glyceraldehyde-3-phosphate dehydrogenase; mRNA: messenger RNA.

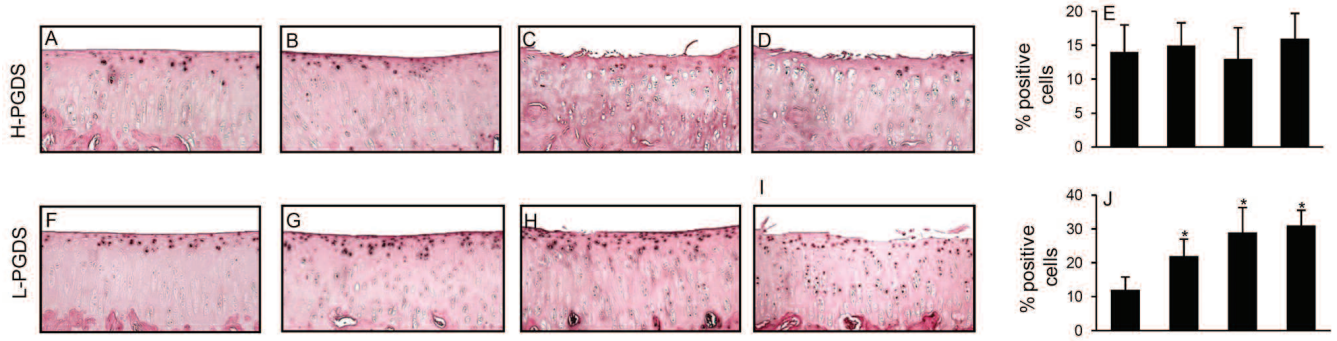

Figure 4. Expression of H-PGDS and L-PGDS during the course of osteoarthritis (OA) in the Hartley guinea pig model. Knee joint sections from 2-, 4-, 8-, and 12-month-old guinea pigs were analyzed by immunohistochemistry for H-PGDS (A, B, C, D) and L-PGDS (F, G, H, I). Control for immunostaining included omitting the primary antibodies, preadsorbing the primary antibodies with a 20-fold molar excess of immunizing antigen, and substituting the primary antibody with nonimmune rabbit IgG (not shown). E, J. Percentage of chondrocytes expressing H-PGDS and L-PGDS during progression of OA in the Hartley guinea pig model. Results are mean ± SD of evaluation of 5 to 10 sections taken from the central region of 5 separate animals. *$p < 0.05$ compared with cartilage from 2-month-old guinea pigs (control). H-PGDS: hematopoietic prostaglandin D synthase; L-PGDS: lipocalin-type PGDS.

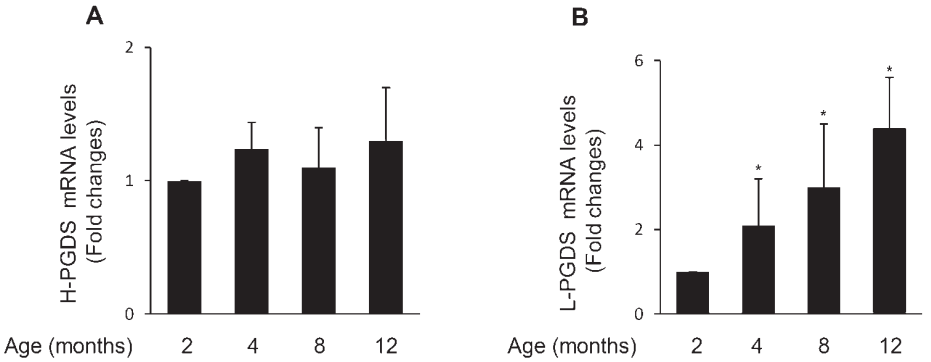

Figure 5. H-PGDS and L-PGDS mRNA expression during the course of OA in the Hartley guinea pig model. Cartilage samples were dissected from medial tibial plateaus of 2-, 4-, 8-, and 12-month-old guinea pigs. Total RNA was isolated, reverse transcribed into cDNA, and H-PGDS (A), L-PGDS (B), and GAPDH mRNA expression was quantified using real-time PCR. All experiments were performed in triplicate and negative controls without template RNA were included in each experiment. Results are expressed as fold change, considering 1 as the value of control (2-mo-old guinea pigs), and are the mean ± SD from 5 separate animals. *$p < 0.05$ compared with cartilage from 2-month-old guinea pigs (control). H-PGDS: hematopoietic prostaglandin D synthase; L-PGDS: lipocalin-type PGDS; mRNA: messenger RNA; GAPDH: glyceraldehyde-3-phosphate dehydrogenase.

Expression of PPAR-α, β, and γ during progression of OA in the ACLT dog model. We investigated the location and expression levels of PPAR-α, β, and γ during the progression of OA in the ACLT dog model. This model mimics joint changes that characterize OA in humans following trauma or injury[36,37]. Results showed that each PPAR isoform was present in normal cartilage (Figure 2F, 2K, and 2P). PPAR-α was mainly expressed in the superficial and middle zones (Figure 2F-2I) and PPAR-β was detected in all zones of cartilage (Figure 2K-2N). However, the levels of PPAR-α and β did not vary at any time postsurgery (Figure 2F-2I and 2K-2N). Thus, these enzymes were constitutively expressed throughout the time course of OA in this model.

PPAR-γ was expressed mainly in the superficial and middle zones in normal cartilage (Figure 2P) and its levels decreased over the course of OA. At 4 weeks postsurgery, the level of PPAR-γ was lower in both superficial and middle zones of cartilage (Figure 2Q) and decreased further at 8 weeks postsurgery (Figure 2R). By 12 weeks after surgery, the levels of PPAR-γ continued to decrease (Figure 2S). The decrease was more marked in the superficial zones (Figure 2S). In some sections, < 5% of cells were stained and the staining was located only in the middle zone. The immunostaining was abolished by preadsorption of the antibody with the antigenic peptide demonstrating its specificity. Real-time PCR analysis revealed that PPAR-γ mRNA levels decreased, whereas PPAR-α and PPAR-β levels did

not change significantly during the course of OA (Figure 6). These findings suggest that the reduction of PPAR-γ expression might be involved in the development of OA.

Expression of H- and L-PGDS during progression of OA in the dog ACLT model. We also analyzed the expression of H- and L-PGDS in cartilage during the development of OA in the ACLT dog model. Our results showed that both L-PGDS and H-PGDS were detectable in the superficial and middle zones of cartilage from non-operated animals (Figure 7A, 7F).

The expression level of H-PGDS did not vary significantly during the progression of disease (Figure 7A-7D). In contrast, L-PGDS levels increased with disease progression (Figure 7F-7I). In normal cartilage, L-PGDS was detected predominantly in the superficial zone of cartilage and the level was relatively low (Figure 7F). At 4 weeks postsurgery, the levels of L-PGDS were significantly higher than in cartilage from non-operated animals (Figure 7G). At 8 weeks postsurgery, the level of L-PGDS was elevated in all the zones of cartilage (Figure 7H), continued to increase with disease progression, and remained elevated until the end of the study at 12 weeks (Figure 7I). Control sections showed no staining (data not shown). As shown in Figure 8, the pattern of mRNA changes of H- and L-PGDS were similar to those of H- and L-PGDS protein changes. These data suggest that the upregulation of L-PGDS expression might be part of an adaptive mechanism to counterbalance increased inflammatory and catabolic responses.

Correlations between histological score and expression levels of PPAR-γ and L-PGDS. Correlation analysis was performed to determine whether the levels of PPAR-γ or L-PGDS in cartilage were associated with histological grade

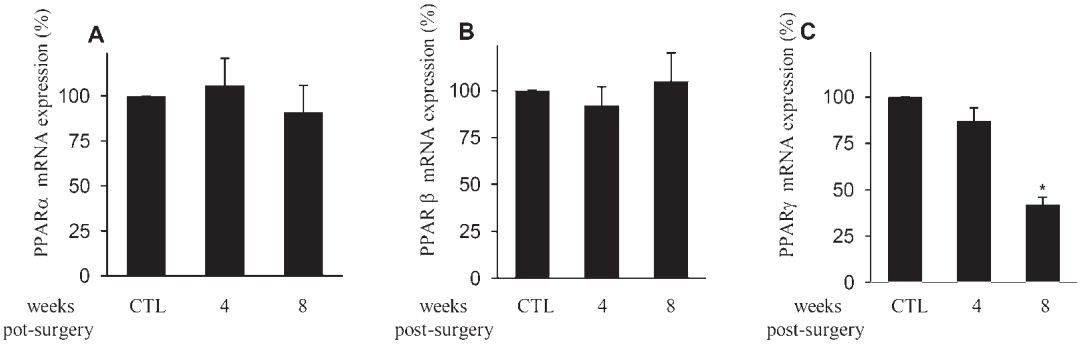

Figure 6. PPAR-α, PPAR-β, and PPAR-γ mRNA expression during the course of osteoarthritis in the ACLT dog model. Cartilage samples were dissected from weight-bearing areas of tibial plateaus of normal (control) and operated dogs at 4 and 8 weeks postsurgery. Total RNA was isolated, reverse transcribed into cDNA, and PPAR-α (A), PPAR-β (B), PPAR-γ (C), and GAPDH mRNA expression was quantified using real-time PCR. All experiments were performed in triplicate and negative controls without template RNA were included in each experiment. Results are expressed as fold changes compared to control (non-operated dogs) and are the mean ± SD from 4 separate animals. *$p < 0.05$ compared with cartilage from non-operated dogs (control). PPAR: peroxisome proliferator-activated receptors; ACLT: anterior cruciate ligament transection; mRNA: messenger RNA; GAPDH: glyceraldehyde-3-phosphate dehydrogenase.

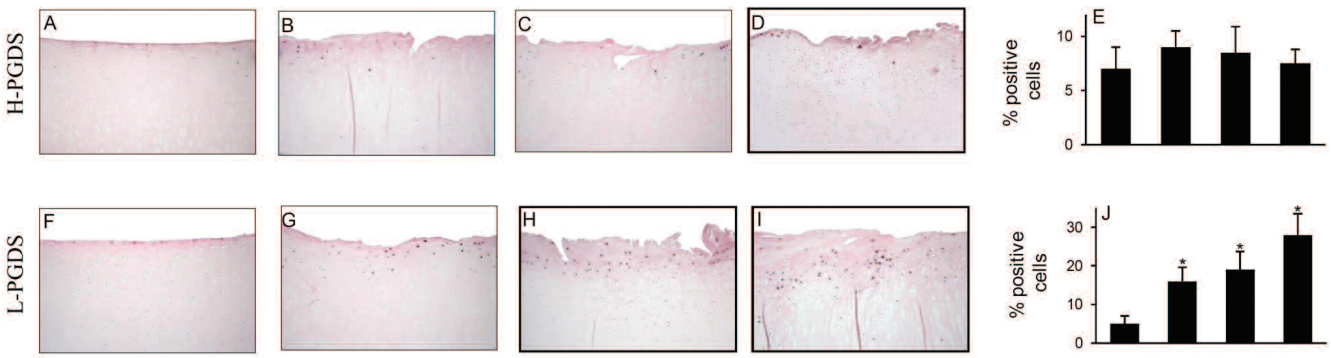

Figure 7. Expression of H-PGDS and L-PGDS in cartilage during the course of osteoarthritis in the ACLT dog model. Cartilage sections from weight-bearing areas of tibial plateaus of normal (control) and operated dogs at 4, 8, 10, and 12 weeks postsurgery were analyzed by immunohistochemistry for H-PGDS (A, B, C, D) and L-PGDS (E, F, G, H). Control for immunostaining included preadsorbing primary antibodies with 20-fold molar excess of immunizing antigen and substituting the primary antibody with nonimmune rabbit IgG (not shown). E, J. Percentage of chondrocytes expressing H-PGDS and L-PGDS during progression of OA in the ACLT dog model. Results are mean ± SD of evaluation of 5 to 10 sections taken from 4 separate animals. *$p < 0.05$ compared with cartilage from non-operated dogs (control). H-PGDS: hematopoietic prostaglandin D synthase; L-PGDS: lipocalin-type PGDS; ACLT: anterior cruciate ligament transection.

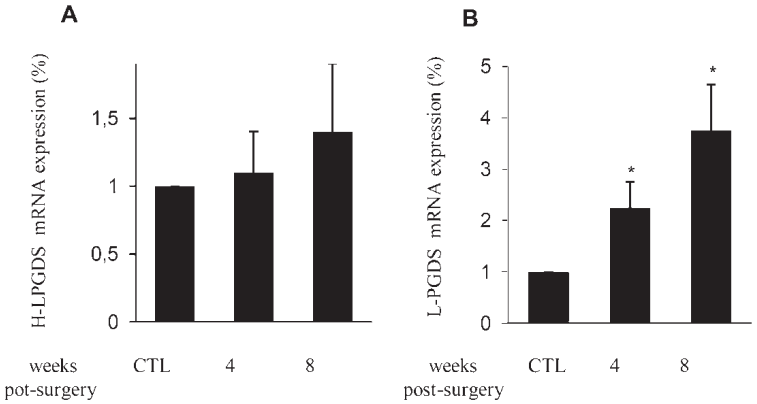

Figure 8. H-PGDS and L-PGDS mRNA expression in cartilage during progression of osteoarthritis in the ACLT dog model. Cartilage samples were dissected from weight-bearing areas of tibial plateaus of normal (control) and operated dogs at 4 and 8 weeks postsurgery. Total RNA was isolated, reverse transcribed into cDNA, and H-PGDS (A), L-PGDS (B), and GAPDH mRNA expression was quantified using real-time PCR. All experiments were performed in triplicate and negative controls without template RNA were included in each experiment. Results are expressed as fold changes compared to control (non-operated dogs) and are mean ± SD from 4 separate animals. *$p < 0.05$ compared with cartilage from non-operated dogs (control). H-PGDS: hematopoietic prostaglandin D synthase; L-PGDS: lipocalin-type PGDS; ACLT: anterior cruciate ligament transection; mRNA: messenger RNA; GAPDH: glyceraldehyde-3-phosphate dehydrogenase.

of OA in guinea pigs and dogs. As shown in Figure 9, the levels of PPAR-γ correlated negatively ($r = –0.77$, $p < 0.05$; Figure 9A), whereas the levels of L-PGDS correlated positively ($r = 0.66$, $p < 0.05$; Figure 9B) with the histological grade of OA in the spontaneous guinea pig model. There was also a negative correlation between PPAR-γ levels ($r = –0.75$, $p < 0.05$; Figure 9C) and a positive correlation between L-PGDS levels ($r = 0.78$, $p < 0.05$; Figure 9D) and the histological grade of OA in the ACLT dog model.

PPAR-γ silencing enhanced basal and IL-1-induced MMP-13 and NO production in human chondrocytes. To further define the influence of PPAR-γ downregulation during OA, we investigated the effect of its silencing by siRNA on basal and IL-1β-induced production of an inflammatory and a catabolic marker of OA, namely NO and MMP-13, respectively. Chondrocytes were transfected with the scrambled control siRNA or PPAR-γ siRNA, and after 48 h of transfection, the cells were left untreated or were stimulated with IL-1β (100 pg/ml) for 24 h. The levels of MMP-13 protein and nitrites in the conditioned media were determined by ELISA and Griess reagent, respectively. As shown in Figure 10A, transfection with the PPAR-γ siRNA enhanced basal production of both NO and MMP-13 (Figure 10A). Similarly, PPAR-γ silencing enhanced IL-1β-induced production of MMP-13 and NO production (Figure 9B). In contrast, transfection with scrambled control siRNA had no effect. PPAR-γ protein levels were reduced by as much as 80%–85%, confirming gene silencing (Figure 10, lower panels). These data indicate that PPAR-γ downregulation increased MMP-13 and NO production and confirm its anti-OA properties.

L-PGDS overexpression decreased basal and IL-1-induced MMP-13 and NO production in human chondrocytes. We also investigated the effect of ectopic expression of L-PGDS on basal and IL-1-induced MMP-13 and NO production in human OA chondrocytes. Chondrocytes were transiently transfected with either an expression vector for human L-PGDS (FLAG-tagged L-PGDS) or the parental empty vector, and at 48 h posttransfection the cells were reincubated in the absence or presence of IL-1 (100 pg/ml) for an additional 24 h, and the levels of nitrites and MMP-13 were measured in conditioned media. As shown in Figure 11, L-PGDS overexpression decreased basal (Figure 11A) and IL-1-induced (Figure 11B) NO and MMP-13 production. Western blotting analysis using anti-FLAG antibody revealed the presence of L-PGDS in FLAG-tagged L-PGDS-transfected cells. In contrast, no signal was detected in nontransfected or empty-vector-transfected cells (Figure 11, lower panels). Moreover, Western blotting with an anti-L-PGDS antibody revealed the presence of L-PGDS in nontransfected and empty-vector-transfected cells and a stronger signal in FLAG-tagged L-PGDS-transfected cells, confirming gene overexpression (Figure 11, lower panels). As determined by the trypan blue exclusion assay, the viability of the empty-vector-transfected cells was similar to that of L-PGDS-transfected cells, indicating that L-PGDS overexpression did not affect chondrocyte viability (data not

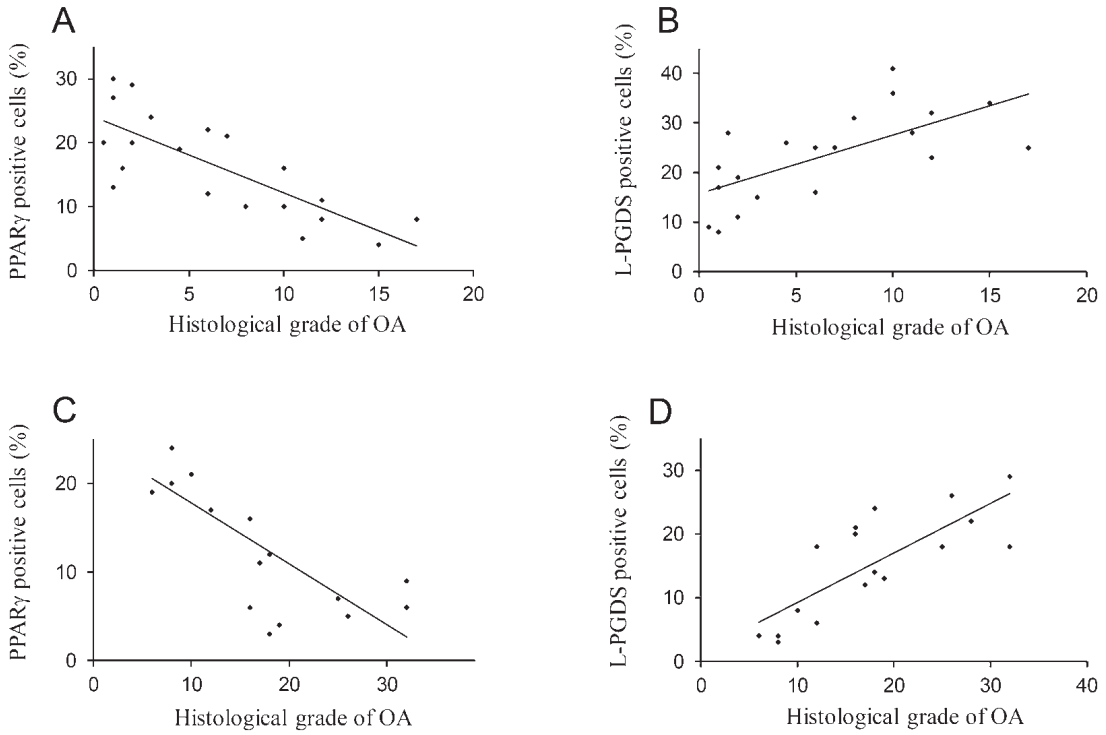

Figure 9. Correlation between levels of PPAR-γ and L-PGDS and histologic grade of osteoarthritis (OA) in the Hartley guinea pig and the ACLT dog model. PPAR-γ levels in cartilage correlated negatively ($r = -0.77$, $p < 0.05$), whereas L-PGDS levels correlated positively ($r = 0.66$, $p < 0.05$) with the histological grade of OA in the Hartley guinea pig model (A, B). There was also a negative correlation between PPAR-γ levels ($r = -0.75$, $p < 0.05$) and a positive correlation between L-PGDS levels ($r = 0.78$, $p < 0.05$) and histological grade of OA in the ACLT dog model (C, D). PPAR: peroxisome proliferator-activated receptors; L-PGDS: lipocalin-type prostaglandin D synthase; ACLT: anterior cruciate ligament transection.

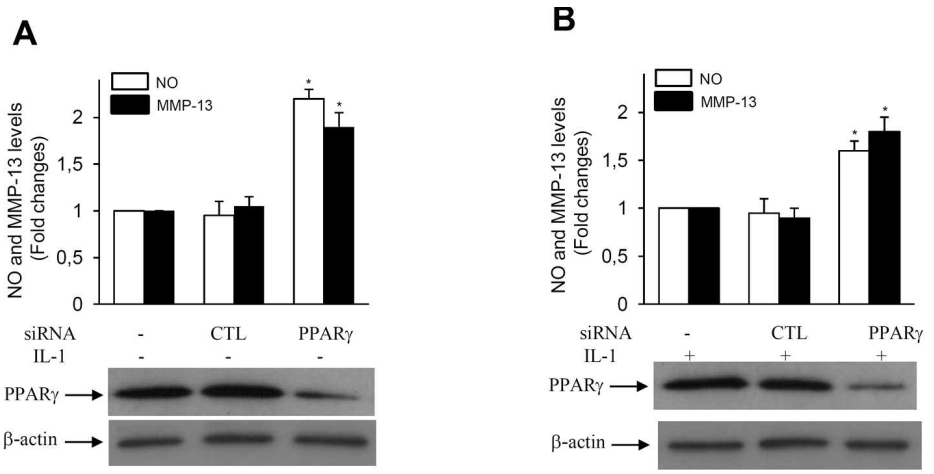

Figure 10. PPAR-γ silencing enhanced basal and IL-1-induced production of NO and MMP-13 in human chondrocytes. Cells were transfected with 100 nM of scrambled control siRNA or PPAR-γ siRNA. At 24 h posttransfection, cells were washed, reincubated another 24 h, and left untreated (A) or treated with 100 pg/ml IL-1 for 24 h (B). Levels of MMP-13 protein and nitrites in the conditioned media were determined by ELISA and Griess reagent, respectively. Results are expressed as fold changes considering 1 as the value of nontransfected cells, and represent mean ± SD of 4 independent experiments. *$p < 0.05$ compared with nontransfected cells. Lower panels: cell lysates were prepared and analyzed for PPAR-γ protein expression by Western blotting. Blots were stripped and reprobed with a specific anti-β-actin antibody. Blots are representative of similar results obtained from 4 independent experiments. PPAR: peroxisome proliferator-activated receptors; MMP: matrix metalloproteinases; IL: interleukin; siRNA: small interfering RNA.

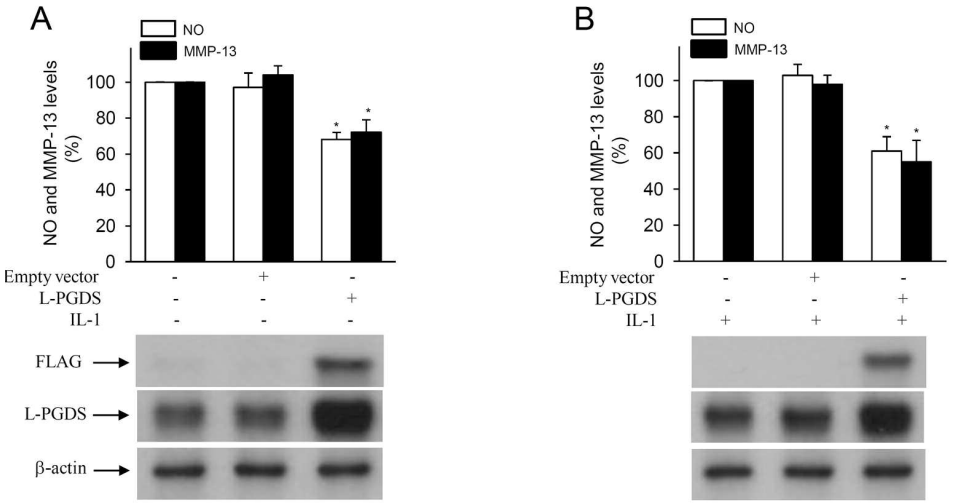

Figure 11. L-PGDS overexpression decreased basal and IL-1-induced production of NO and MMP-13 in human chondrocytes. Cells were transfected with 1 μg of empty vector or FLAG-tagged L-PGDS. At 8 h posttransfection, cells were washed, reincubated another 40 h, then left untreated (A) or treated with 100 pg/ml IL-1 for 24 h (B). Levels of MMP-13 protein and nitrite/nitrate in the conditioned media were determined by ELISA and Griess reagent, respectively. Results are expressed as percentage of control, considering 100% as the value of nontransfected cells, and represent mean ± SD of 4 independent experiments. *$p < 0.05$ compared with nontransfected cells. Lower panels: cell lysates were prepared and analyzed by Western blotting with anti-FLAG, anti-L-PGDS, and anti-β-actin antibodies. Blots are representative of similar results obtained from 4 independent experiments. L-PGDS: lipocalin-type prostaglandin D synthase; IL: interleukin; MMP: matrix metalloproteinases.

shown). These data indicated that L-PGDS overexpression inhibits NO and MMP-13 release in human chondrocytes, further supporting its anti-OA effects *in vivo*.

DISCUSSION

We investigated the expression of PPAR-α, β, and γ, and H-PGDS and L-PGDS in knee joint cartilage during the progression of OA in the spontaneous Hartley guinea pig model and in the ACLT dog model. We report for the first time, to our knowledge, that expression of PPAR-γ protein decreased, whereas the level of L-PGDS increased during the course of OA in both models. In contrast, the levels of PPAR-α and PPAR-β and H-PGDS did not change. Given the roles of PPAR-γ and L-PGDS, these data suggest that decreased PPAR-γ expression may be involved in the pathogenesis of OA, whereas increased expression of L-PGDS may be part of an attempted reparative process.

Considerable evidence indicates that PPAR-γ has protective properties in OA. Indeed, PPAR-γ activation inhibits the production of several inflammatory and catabolic mediators by chondrocytes and other articular joint cells[14,15,16,17,18,19,20,21,22,23,24,25]. In addition, PPAR-γ activators have been tested successfully in animal models of OA[26,27]. However, the expression pattern of PPAR-γ in cartilage during the course of OA is unknown. Our study demonstrated that normal cartilage from 2-month-old guinea pigs expressed PPAR-α, β, and γ. Expression of PPAR-α was moderate to strong, and was located throughout the 3 zones of cartilage. Expression of PPAR-β and γ was weak to moderate, and was located predominantly in the superficial and middle zones. No changes in PPAR-α or β levels were detected in OA cartilage at any time period studied. By contrast, PPAR-γ levels decreased with age and correlated negatively with the severity of histological damage from 4 to 12 months of age in the Hartley guinea pigs. Similarly, in the ACLT dog model, normal cartilage expressed each PPAR isoform. While the expression of PPAR-α and β remained unchanged, the expression of PPAR-γ decreased with the progression of OA, and was lowest at 12 weeks postsurgery. The reduced expression of PPAR-γ was not a consequence of reduced cellularity, because the levels of PPAR-α and β did not change with progression of OA. It is noteworthy that the histological changes we observed are consistent with previous findings in both the Hartley guinea pig model[38,39] and the ACLT dog model[40,41]. Importantly, the observed reduction in PPAR-γ expression correlated negatively with histological OA scores in both disease models.

These results are consistent with the findings of Dumond, *et al*, who reported reduced PPAR-γ expression in cartilage from a rat model of mono-iodoacetate-induced OA[42]. Similarly, Watters, *et al* described reduced expression of PPAR-γ during progression of OA in the spontaneous STR/Ort mouse model[43]. Moreover, we have previously

demonstrated that the levels of PPAR-γ were reduced in human OA compared to normal cartilage[31]. Hence, considering the antiarthritic properties of PPAR-γ, these data strongly suggest that reduction in PPAR-γ expression may be implicated in the pathogenesis of OA.

Several mechanisms may be involved in the decreased expression of PPAR-γ during OA. The most likely is inflammation. Indeed, we and others have shown that inflammatory mediators known to be elevated in OA joints, such as IL-1, IL-17, TNF-α, and PGE_2, downregulate PPAR-γ expression in several cell types including cultured chondrocytes[17,31]. Moreover, TNF-α was reported to induce PPAR-γ cleavage through activation of the caspase cascade in adipocytes[44]. A second mechanism that may be responsible for diminished levels of PPAR-γ could be mechanical stress, a known risk factor for knee OA. In this context, reports have shown a negative effect of mechanical and shear stress on PPAR-γ expression[45,46]. Alternatively, PPAR-γ downregulation could be mediated by hypoxia-inducible factor, which has been shown to have a negative effect on PPAR-γ[47], and levels of hypoxia-inducible factor are elevated in OA[48].

Whereas the expression of PPAR-γ decreased over the progression of OA, levels of PPAR-α and β did not change, suggesting that PPAR-α and β do not play significant roles in the pathogenesis of OA. The role of PPAR-α in OA is controversial. In some studies, PPAR-α activation was shown to prevent IL-1-induced proteoglycan degradation, gelatinolytic activity, and expression of MMP-1, 3 and 13, and to enhance production of IL-1 receptor antagonist[49]. Moreover, PPAR-α activation reduces transforming growth factor-β-induced proteoglycan synthesis[50]. In contrast, in other studies, activation of PPAR-α had no effect on inflammatory or catabolic responses in chondrocytes such as the IL-1-induced production of NO, MMP-1, and MMP-13[14], IL-1-mediated proteoglycan degradation[17], and lipopolysaccharide-induced expression of the acute-phase protein lipocalin-2/SIP[51]. Further studies are clearly warranted to define the role of PPAR-α in the regulation of inflammatory and catabolic responses in chondrocytes and in the pathogenesis of OA.

We investigated the expression of L- and H-PGDS, which catalyze biosynthesis of the endogenous PPAR-γ ligand 15d-PGJ_2. We found that L-PGDS levels increased during the course of OA. In the spontaneous Hartley guinea pig model, the level of L-PGDS was low at age 2 months and had increased significantly at 4 months. Levels increased again from 4 months to 8 months, and remained consistently elevated thereafter to 12 months of age. Similarly, in the ACLT dog model, a significant increase in the level of L-PGDS was observed at Week 4 postsurgery, peaking at Week 8, and then remained at maximal levels by Week 12 postsurgery. These findings are consistent with our previous results showing that the level of L-PGDS was elevated in human OA cartilage compared with normal cartilage[52]. The increased expression of L-PGDS in OA cartilage is likely to be mediated by IL-1β, because exposure to IL-1β enhanced L-PGDS expression in human chondrocytes in a time- and dose-dependent manner[52]. Correlation analysis revealed that the increased expression of L-PGDS correlated positively with OA histological score. Given the antiinflammatory and anticatabolic effects of L-PGDS metabolites[14,15,16,17,18,19,20,21,22,23,24,25,26,27], it is tempting to speculate that increased expression may be part of a negative feedback control of inflammatory and catabolic responses during OA. It is notable that the observed upregulation of L-PGDS, which catalyzes biosynthesis of the most potent PPAR-γ activator, 15d-PGJ_2, proceeds in parallel with downregulation of PPAR-γ. Thus, it is possible that upregulation of L-PGDS may represent a compensatory mechanism against reduced PPAR-γ expression.

In contrast to L-PGDS, levels of H-PGDS remained unchanged during the progression of OA in both disease models, suggesting that this pathway does not play a significant role in the pathogenesis of OA. However, it is important to highlight that although H-PGDS levels did not change during OA, one cannot exclude the possibility that the enzymatic activity was modulated, leading to altered levels of 15d-PGJ_2. In this context, one limitation of our study is the lack of data on 15d-PGJ_2 levels in cartilage or synovial fluid. Such quantification may have provided a more sensitive measure of the activity of these enzymes during OA.

It is notable that the increased level of L-PGDS in cartilage was more pronounced and the decreased expression of PPAR-γ was more intense in the ACLT dog model than in the spontaneous guinea pig model. This is likely due to differences in the microenvironments of articular cartilage in the 2 models. Indeed, there are differences in the mechanisms underlying the pathogenesis of naturally occurring and surgically induced OA in guinea pigs[36,53], dogs[54], and mice[55]. For instance, surgically induced OA involves more joint inflammation than spontaneous OA, with elevated levels of the proinflammatory cytokines IL-1 and TNF-α[36,53,56]. Interestingly, these 2 cytokines were shown to downregulate PPAR-γ[31,44] and to upregulate L-PGDS expression[52,57]. Mapp, *et al* compared osteochondral and synovial angiogenesis in the spontaneous guinea pig model and the surgical rat model, and found that surgical OA reproducibly displays osteochondral and synovial angiogenesis, whereas the guinea pig model displays low vascularity throughout the course of OA[58]. Thus, it is also possible that increased levels of angiogenic factors in the surgical model may be responsible for the pronounced changes in PPAR-γ and L-PGDS expression. In this context, vascular endothelial growth factor (VEGF) was demonstrated to enhance L-PGDS[57] and to reduce PPAR-γ

expression[59]. Further studies are clearly warranted to define the mechanisms that regulate L-PGDS and PPAR-γ expression in spontaneous and surgically induced OA.

Using human cultured chondrocytes, we demonstrated that PPAR-γ silencing enhanced NO and MMP-13 production, confirming that PPAR-γ has antiinflammatory and anticatabolic properties and could be protective in OA. This is in agreement with studies from Setoguchi, *et al*[60] showing that arthritis is exacerbated in mice heterozygous for PPAR-γ deficiency. We also demonstrated that L-PGDS overexpression reduced MMP-13 and NO production in human OA chondrocytes. This is consistent with the findings of Wang, *et al* showing that ectopic expression of L-PGDS in T/C-28a2 chondrocytes inhibits production of IL-6 and activation of nuclear factor-κB[61]. Together with the observed changes in PPAR-γ and L-PGDS levels during the course of OA in the dog and guinea pig models, these findings suggest that PPAR-γ downregulation may contribute to the pathogenesis of OA, whereas increased expression of L-PGDS may be part of a reparative mechanism.

Our results showed decreased expression of PPAR-γ and increased expression of L-PGDS during the course of OA. Further studies are needed to evaluate whether the reduced expression of PPAR-γ is an underlying cause of OA, whether the upregulation of L-PGDS is a repair response, and whether this applies to humans. Our results also suggest that these pathways may be molecular targets for directed therapy in OA.

ACKNOWLEDGMENT

The authors thank Virginia Wallis for assistance with manuscript preparation.

REFERENCES

1. Kapoor M, Martel-Pelletier J, Lajeunesse D, Pelletier JP, Fahmi H. Role of proinflammatory cytokines in the pathophysiology of osteoarthritis. Nat Rev Rheumatol 2011;7:33-42.
2. Goldring MB, Marcu KB. Cartilage homeostasis in health and rheumatic diseases. Arthritis Res Ther 2009;11:224.
3. de Lange-Brokaar BJ, Ioan-Facsinay A, van Osch GJ, Zuurmond AM, Schoones J, Toes RE, et al. Synovial inflammation, immune cells and their cytokines in osteoarthritis: A review. Osteoarthritis Cartilage 2012;20:1484-99.
4. Abbott BD. Review of the expression of peroxisome proliferator-activated receptors alpha (PPAR alpha), beta (PPAR beta), and gamma (PPAR gamma) in rodent and human development. Reprod Toxicol 2009;27:246-57.
5. Fruchart JC. Peroxisome proliferator-activated receptor-alpha (PPAR-alpha): At the crossroads of obesity, diabetes and cardiovascular disease. Atherosclerosis 2009;205:1-8.
6. Michalik L, Wahli W. Peroxisome proliferator-activated receptors (PPARs) in skin health, repair and disease. Biochim Biophys Acta 2007;1771:991-8.
7. Hall MG, Quignodon L, Desvergne B. Peroxisome proliferator-activated receptor beta/delta in the brain: Facts and hypothesis. PPAR Res 2008;2008:780452.
8. Szanto A, Nagy L. The many faces of PPAR-gamma: Anti-inflammatory by any means? Immunobiology 2008; 213:789-803.
9. Cho MC, Lee K, Paik SG, Yoon DY. Peroxisome proliferators-activated receptor (PPAR) modulators and metabolic disorders. PPAR Res 2008;2008:679137.
10. Fahmi H, Martel-Pelletier J, Pelletier JP, Kapoor M. Peroxisome proliferator-activated receptor gamma in osteoarthritis. Mod Rheumatol 2011;21:1-9.
11. Kliewer SA, Lenhard JM, Willson TM, Patel I, Morris DC, Lehmann JM. A prostaglandin J2 metabolite binds peroxisome proliferator-activated receptor gamma and promotes adipocyte differentiation. Cell 1995;83:813-9.
12. Forman BM, Tontonoz P, Chen J, Brun RP, Spiegelman BM, Evans RM. 15-Deoxy-delta 12, 14-prostaglandin J2 is a ligand for the adipocyte determination factor PPAR gamma. Cell 1995;83:803-12.
13. Urade Y, Eguchi N. Lipocalin-type and hematopoietic prostaglandin D synthases as a novel example of functional convergence. Prostaglandins Other Lipid Mediat 2002;68-69:375-82.
14. Fahmi H, Di Battista JA, Pelletier JP, Mineau F, Ranger P, Martel-Pelletier J. Peroxisome proliferator-activated receptor gamma activators inhibit interleukin-1 beta-induced nitric oxide and matrix metalloproteinase 13 production in human chondrocytes. Arthritis Rheum 2001;44:595-607.
15. Fahmi H, Pelletier JP, Mineau F, Martel-Pelletier J. 15d-PGJ(2) is acting as a 'dual agent' on the regulation of COX-2 expression in human osteoarthritic chondrocytes. Osteoarthritis Cartilage 2002;10:845-8.
16. Boyault S, Simonin MA, Bianchi A, Compe E, Liagre B, Mainard D, et al. 15-Deoxy-delta12,14-PGJ2, but not troglitazone, modulates IL-1 beta effects in human chondrocytes by inhibiting NF-kappa B and AP-1 activation pathways. FEBS Lett 2001;501:24-30.
17. Bordji K, Grillasca JP, Gouze JN, Magdalou J, Schohn H, Keller JM, et al. Evidence for the presence of peroxisome proliferator-activated receptor (PPAR) alpha and gamma and retinoid Z receptor in cartilage. PPARgamma activation modulates the effects of interleukin-1-beta on rat chondrocytes. J Biol Chem 2000;275:12243-50.
18. Boyault S, Bianchi A, Moulin D, Morin S, Francois M, Netter P, et al. 15-Deoxy-delta(12,14)-prostaglandin J(2) inhibits IL-1 beta-induced IKK enzymatic activity and I kappa B alpha degradation in rat chondrocytes through a PPAR gamma-independent pathway. FEBS Lett 2004;572:33-40.
19. Li X, Afif H, Cheng S, Martel-Pelletier J, Pelletier JP, Ranger P, et al. Expression and regulation of microsomal prostaglandin E synthase-1 in human osteoarthritic cartilage and chondrocytes. J Rheumatol 2005;32:887-95.
20. Moulin D, Poleni PE, Kirchmeyer M, Sebillaud S, Koufany M, Netter P, et al. Effect of peroxisome proliferator activated receptor (PPAR) gamma agonists on prostaglandins cascade in joint cells. Biorheology 2006;43:561-75.
21. Bianchi A, Moulin D, Sebillaud S, Koufany M, Galteau MM, Netter P, et al. Contrasting effects of peroxisome-proliferator-activated receptor (PPAR) gamma agonists on membrane-associated prostaglandin E2 synthase-1 in IL-1 beta-stimulated rat chondrocytes: Evidence for PPAR gamma-independent inhibition by 15-deoxy-delta12,14 prostaglandin J2. Arthritis Res Ther 2005;7:R1325-37.
22. Francois M, Richette P, Tsagris L, Raymondjean M, Fulchignoni-Lataud MC, Forest C, et al. Peroxisome proliferator-activated receptor-gamma down-regulates chondrocyte matrix metalloproteinase-1 via a novel composite element. J Biol Chem 2004;279:28411-8.
23. Sabatini M, Bardiot A, Lesur C, Moulharat N, Thomas M, Richard I, et al. Effects of agonists of peroxisome proliferator-activated

receptor gamma on proteoglycan degradation and matrix metalloproteinase production in rat cartilage in vitro. Osteoarthritis Cartilage 2002;10:673-9.
24. Mix KS, Coon CI, Rosen ED, Suh N, Sporn MB, Brinckerhoff CE. Peroxisome proliferator-activated receptor-gamma-independent repression of collagenase gene expression by 2-cyano-3, 12-dioxooleana-1,9-dien-28-oic acid and prostaglandin 15-deoxy-delta(12,14) J2: A role for Smad signaling. Mol Pharmacol 2004;65:309-18.
25. Chabane N, Zayed N, Benderdour M, Martel-Pelletier J, Pelletier JP, Duval N, et al. Human articular chondrocytes express 15-lipoxygenase-1 and -2: Potential role in osteoarthritis. Arthritis Res Ther 2009;11:R44.
26. Boileau C, Martel-Pelletier J, Fahmi H, Mineau F, Boily M, Pelletier JP. The peroxisome proliferator-activated receptor gamma agonist pioglitazone reduces the development of cartilage lesions in an experimental dog model of osteoarthritis: In vivo protective effects mediated through the inhibition of key signaling and catabolic pathways. Arthritis Rheum 2007;56:2288-98.
27. Kobayashi T, Notoya K, Naito T, Unno S, Nakamura A, Martel-Pelletier J, et al. Pioglitazone, a peroxisome proliferator-activated receptor gamma agonist, reduces the progression of experimental osteoarthritis in guinea pigs. Arthritis Rheum 2005;52:479-87.
28. Pelletier JP, Jovanovic D, Fernandes JC, Manning P, Connor JR, Currie MG, et al. Reduced progression of experimental osteoarthritis in vivo by selective inhibition of inducible nitric oxide synthase. Arthritis Rheum 1998;41:1275-86.
29. Kraus VB, Huebner JL, DeGroot J, Bendele A. The OARSI histopathology initiative — Recommendations for histological assessments of osteoarthritis in the guinea pig. Osteoarthritis Cartilage 2010;18 Suppl 3:S35-52.
30. Cook JL, Kuroki K, Visco D, Pelletier JP, Schulz L, Lafeber FP. The OARSI histopathology initiative — Recommendations for histological assessments of osteoarthritis in the dog. Osteoarthritis Cartilage 2010;18 Suppl 3:S66-79.
31. Afif H, Benderdour M, Mfuna-Endam L, Martel-Pelletier J, Pelletier JP, Duval N, et al. Peroxisome proliferator-activated receptor gamma 1 expression is diminished in human osteoarthritic cartilage and is downregulated by interleukin-1 beta in articular chondrocytes. Arthritis Res Ther 2007;9:R31.
32. Fujimori K, Fukuhara A, Inui T, Allhorn M. Prevention of paraquat-induced apoptosis in human neuronal SH-SY5Y cells by lipocalin-type prostaglandin D synthase. J Neurochem 2012;120:279-91.
33. Bendele AM, Hulman JF. Spontaneous cartilage degeneration in guinea pigs. Arthritis Rheum 1988;31:561-5.
34. Bendele AM, White SL, Hulman JF. Osteoarthrosis in guinea pigs: Histopathologic and scanning electron microscopic features. Lab Anim Sci 1989;39:115-21.
35. Watson PJ, Carpenter TA, Hall LD, Tyler JA. Cartilage swelling and loss in a spontaneous model of osteoarthritis visualized by magnetic resonance imaging. Osteoarthritis Cartilage 1996; 4:197-207.
36. Bendele AM. Animal models of osteoarthritis. J Musculoskelet Neuronal Interact 2001;1:363-76.
37. Visco DM, Hill MA, Widmer WR, Johnstone B, Myers SL. Experimental osteoarthritis in dogs: A comparison of the Pond-Nuki and medial arthrotomy methods. Osteoarthritis Cartilage 1996;4:9-22.
38. Johnson K, Svensson CI, Etten DV, Ghosh SS, Murphy AN, Powell HC, et al. Mediation of spontaneous knee osteoarthritis by progressive chondrocyte ATP depletion in Hartley guinea pigs. Arthritis Rheum 2004;50:1216-25.
39. Huebner JL, Johnson KA, Kraus VB, Terkeltaub RA. Transglutaminase 2 is a marker of chondrocyte hypertrophy and osteoarthritis severity in the Hartley guinea pig model of knee OA. Osteoarthritis Cartilage 2009;17:1056-64.
40. Pelletier JP, Martel-Pelletier J, Altman RD, Ghandur-Mnaymneh L, Howell DS, Woessner JF Jr. Collagenolytic activity and collagen matrix breakdown of the articular cartilage in the Pond-Nuki dog model of osteoarthritis. Arthritis Rheum 1983;26:866-74.
41. Fernandes JC, Martel-Pelletier J, Lascau-Coman V, Moldovan F, Jovanovic D, Raynauld JP, et al. Collagenase-1 and collagenase-3 synthesis in normal and early experimental osteoarthritic canine cartilage: An immunohistochemical study. J Rheumatol 1998;25:1585-94.
42. Dumond H, Presle N, Pottie P, Pacquelet S, Terlain B, Netter P, et al. Site specific changes in gene expression and cartilage metabolism during early experimental osteoarthritis. Osteoarthritis Cartilage 2004;12:284-95.
43. Watters JW, Cheng C, Pickarski M, Wesolowski GA, Zhuo Y, Hayami T, et al. Inverse relationship between matrix remodeling and lipid metabolism during osteoarthritis progression in the STR/Ort mouse. Arthritis Rheum 2007;56:2999-3009.
44. Guilherme A, Tesz GJ, Guntur KV, Czech MP. Tumor necrosis factor-alpha induces caspase-mediated cleavage of peroxisome proliferator-activated receptor gamma in adipocytes. J Biol Chem 2009;284:17082-91.
45. David V, Martin A, Lafage-Proust MH, Malaval L, Peyroche S, Jones DB, et al. Mechanical loading down-regulates peroxisome proliferator-activated receptor gamma in bone marrow stromal cells and favors osteoblastogenesis at the expense of adipogenesis. Endocrinology 2007;148:2553-62.
46. Ameshima S, Golpon H, Cool CD, Chan D, Vandivier RW, Gardai SJ, et al. Peroxisome proliferator-activated receptor gamma (PPAR gamma) expression is decreased in pulmonary hypertension and affects endothelial cell growth. Circ Res 2003;92:1162-9.
47. Yun Z, Maecker HL, Johnson RS, Giaccia AJ. Inhibition of PPAR gamma 2 gene expression by the HIF-1-regulated gene DEC1/Stra13: A mechanism for regulation of adipogenesis by hypoxia. Dev Cell 2002;2:331-41.
48. Grimmer C, Pfander D, Swoboda B, Aigner T, Mueller L, Hennig FF, et al. Hypoxia-inducible factor 1-alpha is involved in the prostaglandin metabolism of osteoarthritic cartilage through up-regulation of microsomal prostaglandin E synthase 1 in articular chondrocytes. Arthritis Rheum 2007;56:4084-94.
49. Francois M, Richette P, Tsagris L, Fitting C, Lemay C, Benallaoua M, et al. Activation of the peroxisome proliferator-activated receptor alpha pathway potentiates interleukin-1 receptor antagonist production in cytokine-treated chondrocytes. Arthritis Rheum 2006;54:1233-45.
50. Poleni PE, Bianchi A, Etienne S, Koufany M, Sebillaud S, Netter P, et al. Agonists of peroxisome proliferators-activated receptors (PPAR) alpha, beta/delta or gamma reduce transforming growth factor (TGF)-beta-induced proteoglycans' production in chondrocytes. Osteoarthritis Cartilage 2007;15:493-505.
51. Ulivi V, Cancedda R, Cancedda FD. 15-deoxy-delta 12,14-prostaglandin J(2) inhibits the synthesis of the acute phase protein SIP24 in cartilage: Involvement of COX-2 in resolution of inflammation. J Cell Physiol 2008;217:433-41.
52. Zayed N, Li X, Chabane N, Benderdour M, Martel-Pelletier J, Pelletier JP, et al. Increased expression of lipocalin-type prostaglandin D2 synthase in osteoarthritic cartilage. Arthritis Res Ther 2008;10:R146.
53. Wei L, Fleming BC, Sun X, Teeple E, Wu W, Jay GD, et al. Comparison of differential biomarkers of osteoarthritis with and without posttraumatic injury in the Hartley guinea pig model. J Orthop Res 2010;28:900-6.
54. Meacock SC, Bodmer JL, Billingham ME. Experimental

osteoarthritis in guinea-pigs. J Exp Pathol 1990;71:279-93.
55. McNulty MA, Loeser RF, Davey C, Callahan MF, Ferguson CM, Carlson CS. Histopathology of naturally occurring and surgically induced osteoarthritis in mice. Osteoarthritis Cartilage 2012;20:949-56.
56. Kammermann JR, Kincaid SA, Rumph PF, Baird DK, Visco DM. Tumor necrosis factor-alpha (TNF-alpha) in canine osteoarthritis: Immunolocalization of TNF-alpha, stromelysin and TNF receptors in canine osteoarthritic cartilage. Osteoarthritis Cartilage 1996;4:23-34.
57. Gallant MA, Samadfam R, Hackett JA, Antoniou J, Parent JL, de Brum-Fernandes AJ. Production of prostaglandin D(2) by human osteoblasts and modulation of osteoprotegerin, RANKL, and cellular migration by DP and CRTH2 receptors. J Bone Miner Res 2005;20:672-81.
58. Mapp PI, Avery PS, McWilliams DF, Bowyer J, Day C, Moores S, et al. Angiogenesis in two animal models of osteoarthritis. Osteoarthritis Cartilage 2008;16:61-9.
59. Liu Y, Berendsen AD, Jia S, Lotinun S, Baron R, Ferrara N, et al. Intracellular VEGF regulates the balance between osteoblast and adipocyte differentiation. J Clin Invest 2012;122:3101-13.
60. Setoguchi K, Misaki Y, Terauchi Y, Yamauchi T, Kawahata K, Kadowaki T, et al. Peroxisome proliferator-activated receptor-gamma haploinsufficiency enhances B cell proliferative responses and exacerbates experimentally induced arthritis. J Clin Invest 2001;108:1667-75.
61. Wang P, Zhu F, Tong Z, Konstantopoulos K. Response of chondrocytes to shear stress: Antagonistic effects of the binding partners Toll-like receptor 4 and caveolin-1. FASEB J 2011;25:3401-15.